J. Fluid Mech. (1968), *vol.* 31, *part* 4, *pp.* 643–655
Printed in Great Britain

The observed motion of a sphere through a short, rotating cylinder of fluid

By T. MAXWORTHY†

Jet Propulsion Laboratory, California Institute of Technology, Pasadena, California

(Received 19 April 1967 and in revised form 29 September 1967)

The drag on a sphere has been measured as it moves through a slightly viscous fluid contained in a rotating cylinder that is short compared to the length of 'Taylor columns' created by the sphere motion. These results suggest that only when inertia effects are very much smaller than both viscous and Coriolis forces are the results of Moore & Saffman (1968) approached. Flow field observations show qualitative agreement with many of the features described in their paper but differ sufficiently to warrant a further, fairly extensive discussion. These differences are characterized by a marked fore and aft asymmetry in the shear layer and boundary-layer flows for all values of the parameters covered by this study.

Introduction

When a body moves along the axis of rotation of a long, rapidly spinning cylinder of water, large, slowly attenuating disturbances are propagated fore and aft to produce columns or 'slugs' of almost stagnant fluid. Such phenomena were first, rather briefly but elegantly, discussed by Taylor (1923) and have since been called 'Taylor columns'. Many authors have since contributed to our theoretical knowledge of these effects, but no convincing quantitative experimental measurements have been made. While attempting to perform such experiments‡ in a *long* cylinder and at relatively low rotation rates, the present author found evidence of a weak interaction between the long fore and aft wakes of a sphere and the end walls of the apparatus. Private communication with Prof. D. Fultz of the University of Chicago indicated that in experiments performed there, in short cylinders, very large interactions between the 'Taylor columns' and the end wall were greatly increasing the drag experienced by the sphere. Recent theoretical work on this interaction by Moore & Saffman (1968)§ has made it necessary to extend the range of Fultz's measurements. These are presented here together with the current view on the nature of the flow field created in this very complicated interaction problem.

† Present address: University of Southern California, Los Angeles.
‡ To be published.
§ Referred to as M–S in that which follows.

Apparatus

Shown in figure 1 is a short cylinder, 40 cm long, 28 cm diameter, which can be spun rapidly by a feedback-controlled, constant-speed, d.c. electric motor. A mechanism to release a buoyant sphere (figure 1 *a*) is affixed in the lower end wall, and the upper end wall is removable. Two sphere sizes were used, a table-tennis ball (1·905 cm radius) and a specially fabricated thin-shelled sphere (3·885 cm radius). Each could be almost completely filled with water, sealed, and their buoyancy force, in water, measured by an elementary application of Archimedes' principle.

One of the spheres was placed in the release mechanism, the upper end plate was fixed in place, and the apparatus spun until the water inside was in solid body rotation. The sphere was released and its time of flight measured between two sets of lines. At very high rotation speeds and low buoyance, the sphere wandered off the axis of rotation. The beginning of such behaviour marked the limit of usefulness of the experiments, since these runs produced drag coefficients somewhat below the general trend of the 'well-behaved' case. For some cases dye was injected into the flow, through the end walls, and its motion studied.

Since some difficulty was encountered in injecting dye in a controlled manner, a sphere which could be towed along the axis of rotation was mounted through the upper plate of the apparatus so that it also rotated with the cylinder (figure 1 *b*). This hollow sphere was filled with dye and glued to a hollow s.s. tube at the open end of which there was a pressure relief valve. The latter could be operated while the apparatus was rotating. This rotating tube was attached, through a rotating bearing, to a square rod and a towing wire pulled around the drive shaft of a 1 rev/min clock motor. Four sphere Reynolds numbers between 3·5 and 28 could be obtained in this way. Various tests could be performed with this controllable apparatus. Dye could be injected at a known location and in small amounts in order to observe the streamline character. Direct velocity measurements could be made using the technique described by Baker (1966). A thin platinum wire (0·0005 in. dia.) was stretched across the tank and observed from two mutually perpendicular directions (see inset on figure 8 *b*, plate 4). The fluid was a dilute solution of the indicator Thymol Blue titrated to its end point. When the wire was pulsed with 6 V d.c., a proton exchange reaction took place at the wire and the solution became locally basic. In the thin cylindrical region around the wire, the indicator turned blue and served to mark a line of particles at a given instant of time. The local flow swept the marked particles away and measured, in principle, the local swirl and axial velocities with respect to the rotating reference frame. Unfortunately, the swirl velocities were so much larger than the axial velocities that no meaningful measurements of the latter could be made because of the large distortions of the dye line caused by the former.

Results and discussion

Drag measurements

The primary results are shown in figures 2 and 3. They are presented in a form to ease comparison with the work of M–S discussed in this issue, and the results

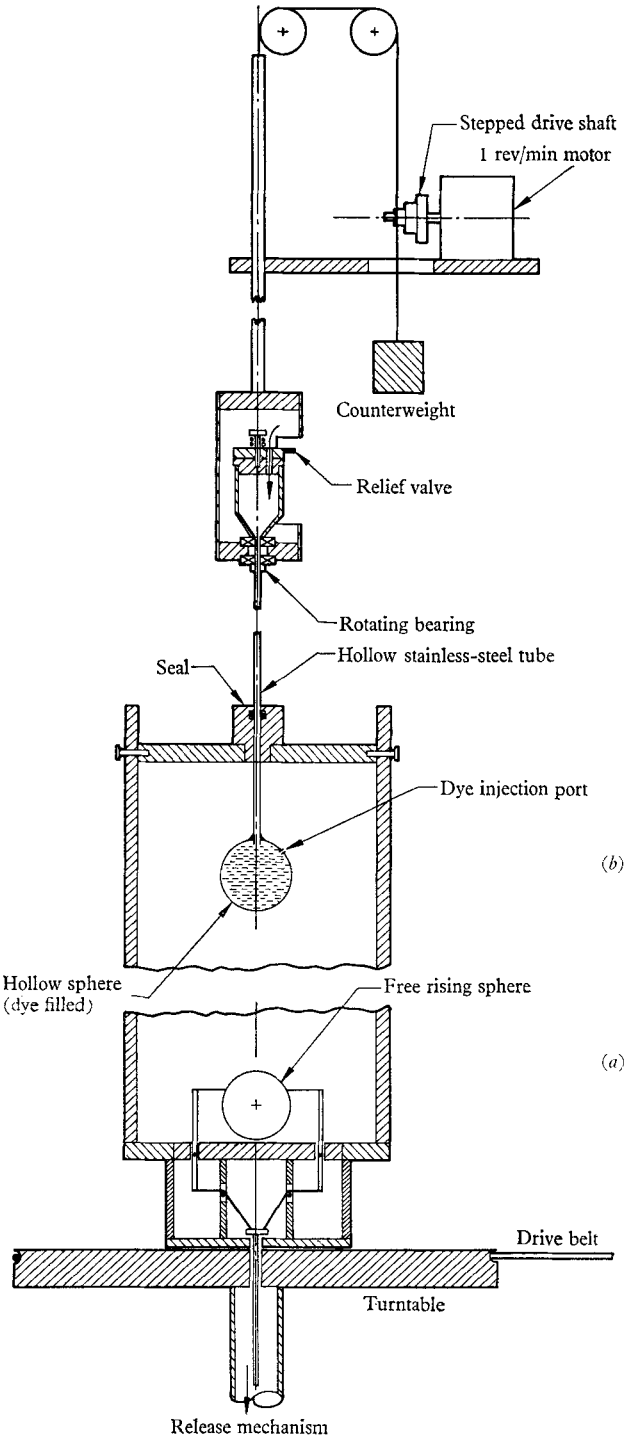

FIGURE 1. (*a*) Apparatus used to measure the velocity of a freely rising sphere. (*b*) Apparatus to tow a captive sphere, introducing dye in known locations and measuring azimuthal velocity profiles.

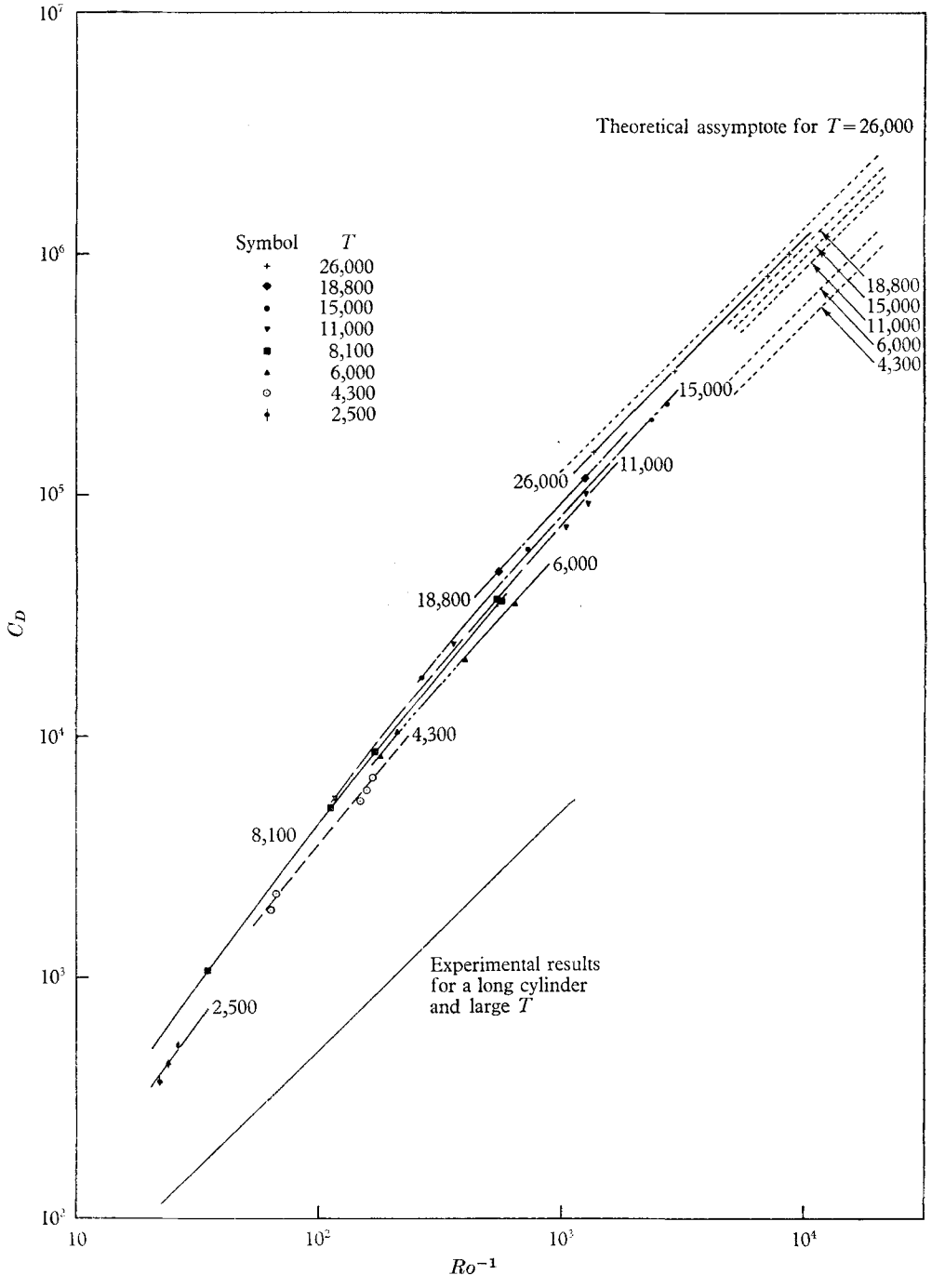

FIGURE 2. Raw data plot of C_D versus $1/Ro$ for various T compared to the theoretical asymptotes of Moore & Saffman (1968) and the experimental results of the present author as found in a long cylinder and large T.

of the present author obtained in a long cylinder; briefly summarized the latter show that as T becomes large and for Ro less than 0·1, C_D is proportional to Ro^{-1} when the small effect of the interaction with the end wall is removed by extrapolation. In the limit described by M–S, $C_D R/T^{\frac{3}{2}}$ is 0·819, for the completely enclosed geometry, where C_D is the drag coefficient, $D/\frac{1}{2}\rho U^2 \pi a^2$; T the Taylor

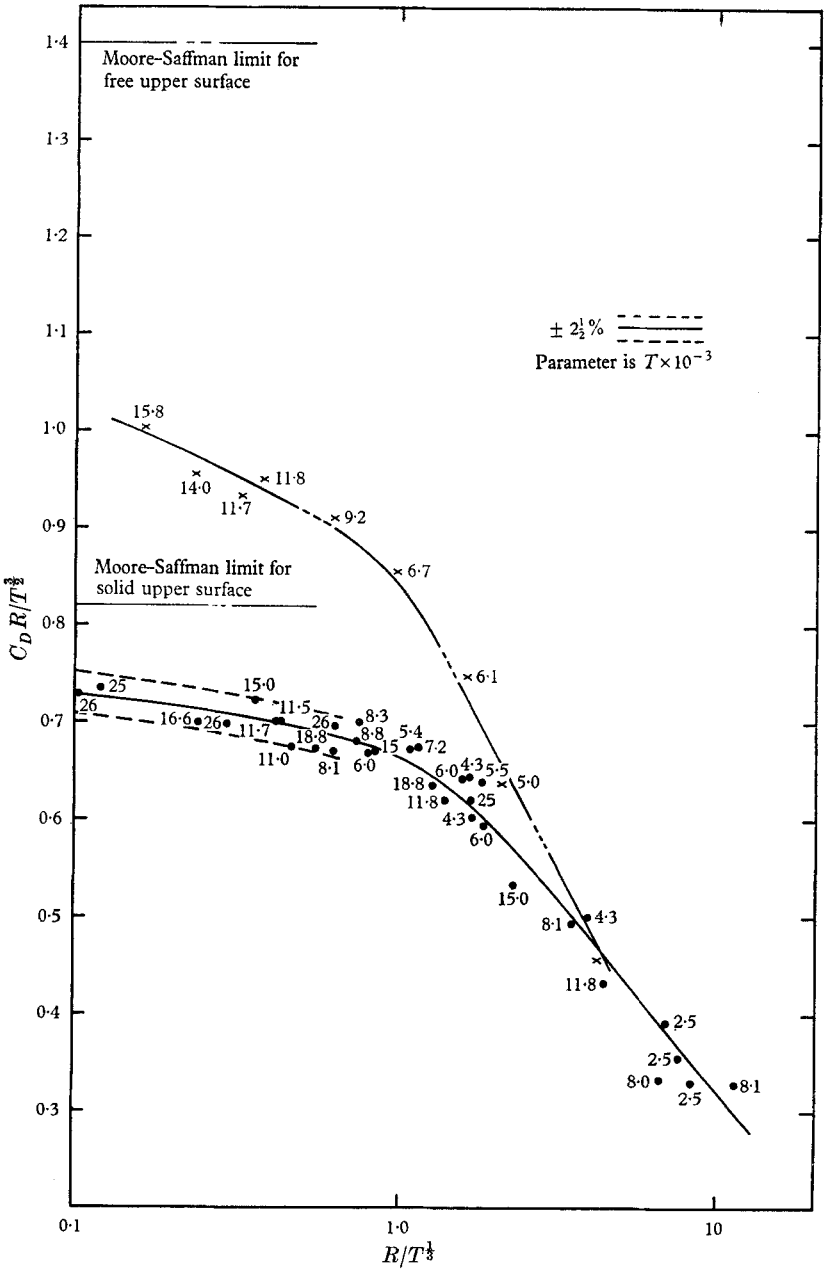

FIGURE 3. $C_D R/T^{\frac{3}{2}}$ versus $R/T^{\frac{1}{3}}$; the best data reduction found to show the approach to results dominated by viscous and Coriolis forces.

number, $\Omega a^2/\nu$; and R the Reynolds number, Ua/ν.† Here D is the drag force or equivalently the buoyancy force, ρ the fluid density and ν its kinematic viscosity, Ω the rate of the basic solid-body rotation and U and a are the velocity and radius of the sphere. In figure 2 we see that when the interaction with the end walls is complete, the drag coefficient increased by one order of magnitude above the case of motion in a long cylinder with no end-wall interaction.

The theoretical considerations of M–S require that the flow be symmetric fore and aft, i.e. no non-linear inertial effects, and that all layers be thin compared to apparatus dimensions. Figure 3 suggests that this is occurring as $R/T^{\frac{1}{3}}$ becomes small. A reasonable extrapolation shows that the theoretical value is approached, to within the accuracy of the experiment ($\pm 2\frac{1}{2}\%$), for values of $R/T^{\frac{1}{3}}$ between 10^{-4} and 10^{-3}, although the slowly varying nature of the results makes it difficult to be certain of the exponent of T for values of $R/T^{\frac{1}{3}}$ smaller than unity, the value at which a transition apparently takes place. It is interesting to rewrite this condition in terms of the inertial parameters of the problem to see how really minute they must be for inertial effects to be negligible; we get $R^2\,Ro$ between 10^{-12} and 10^{-9}! These results tend to confirm the statements of M–S on the limits of validity of their solution. Their most restrictive condition on the importance of inertial effects comes from order-of-magnitude arguments within the shear layers; they require that $R/T^{\frac{2}{7}} \ll a/H^{\frac{3}{7}}$[$O(1)$ in the present case], where H is the height of the cylinder. This result agrees substantially with ours unless $T^{\frac{1}{21}}$ is considerably larger than unity! For the experiments the largest value of this quantity is 1·6 and the results are not accurate enough to tell if this is a significant difference. Since the experimental exponent of $\frac{1}{3}$ was found before the theoretical value of $\frac{2}{7}$ was computed, it is retained even though the theoretical exponent gives a reduction of the data which is as accurate as that shown in figure 3. The order of magnitude is necessarily even smaller in the real case because of the change that takes place within these shear layers as they approach the body. They become very thin and the velocities within them large, so that inertia forces are large there even though they may be small far removed from the body. We must eventually require that inertia forces be small everywhere and a correspondingly lower R and Ro than the M–S restriction is suggested. There are also inertial effects within the forward slug which produce radial flow there, and a further difficulty in the nonuniform character of the boundary-layers found behind the sphere and at the lower boundary. These will be discussed more fully in the following sections.

Also shown in figure 3 are a few results of sphere drag measured when the upper surface, towards which the sphere was moving, was a free surface. For this geometry the theoretical value of $C_D R/T^{\frac{1}{2}}$ is 1·405. Because of this surface's inability to support an Ekman layer, the fluid trapped within the Taylor column must be mainly, though not completely, removed through the Ekman layer on

† It is often convenient to use the inverse of the Taylor number, i.e. $\nu/\Omega a^2$, sometimes called the Ekman number (E), and an inertial measure of the Coriolis force $U/\Omega a$, the Rossby number (Ro). The choice of the parameter used is, as in all such problems, a personal one and seems to defy any rational analysis. Thus it is becoming conventional for the Ekman layer thickness to be written as $O(E^{\frac{1}{2}})$, yet an ordinary boundary layer has thickness $O(R^{-\frac{1}{2}})$!

the sphere surface. This results in an increased vorticity external to the layer and an increased dissipation in the layer. The resultant drag increase is shown clearly in the results, corresponding parametric conditions having around a 35% increase in C_D over the case with both end walls solid. Further work on this phase of the investigation is anticipated for the future. In the present paper we will only briefly mention a few crude observations of the drag and flow field.

The flow field

Dye studies

These were used mainly to try to understand the overall character of the flow field. What do the meridional streamlines, i.e. mass carrying streamlines, look like? Which of the M–S conditions are unrealistic? etc. Visual observation, still and time lapse photography were used to reconstruct the flow field. Several curious phenomena were noted and will be discussed appropriately.

The flow field can be conveniently divided into three parts, the interactions at upper and lower walls and at the sphere. Figure 4 shows the meridional flow field around the sphere under the conditions of most of the experiments. There are quantitative variations from this picture, but in general it qualitatively represents the flow under the low R conditions tested.

Flow ahead of the sphere is relatively uncomplicated. Within the 'Taylor column' the fluid is rotating slower than the sphere; this fluid is smoothly sucked into a thin Ekman layer and passes around the sphere, with no apparent thickening at the equator, to be ejected in a layer behind the sphere (figure 5, plate 1). Since this latter layer is not well behaved and does not resemble the corresponding theoretical Ekman solution, it will be discussed in more detail later. Within the 'almost-geostrophic' forward slug is a small radial flow. A few measurements of the radial velocity of this flow show that it scales approximately with $RT^{-\frac{1}{2}}$†, which is consistent with the assumption that this flow is of inertial origin. Outside of this central region is a jet transporting fluid from the Ekman layer on the upper plate to the rear of the sphere. This layer grows thinner with larger internal axial and azimuthal velocities as it approaches the sphere (figure 6*c*, plate 2). It sweeps around the equator and suddenly jumps to a larger radius. At low Reynolds numbers this seems to be a fairly smooth transition, but at higher Reynolds numbers it looks very much like an annular undular jump phenomenon (figure 7*c*, plate 3) which in rotating fluids has been called a vortex jump (Benjamin 1962). One might speculate that as R decreases still further and inertial forces become smaller than viscous forces, this jump must be smoothed out completely and become symmetric about the equator (cf. the behaviour of very viscous, free surface flow over an obstacle). Outside of this layer there is evidence of another region within which fluid is being recirculated, as shown in figure 4 and the lower right-hand corner of figure 7*b*, plate 3. Unfortunately, the precise specification of this region is ambiguous because dye from the inner layer does not always flow into it and because it suffers an azimuthal instability which makes it difficult to see its true nature. Thus the layer tends to break up into a

† From the results of M–S one finds that inertial effects are negligible when this parameter is much smaller than unity.

varying number of long cells spaced around the circumference of the circumscribing cylinder. These cells move out into the outer flow and cause considerable disturbance there. Depending on circumstances, there may be between 2 and 6 of these cells, and at low T and/or large R they penetrate into the interior regions of the flow (figure 8*a*, plate 4).

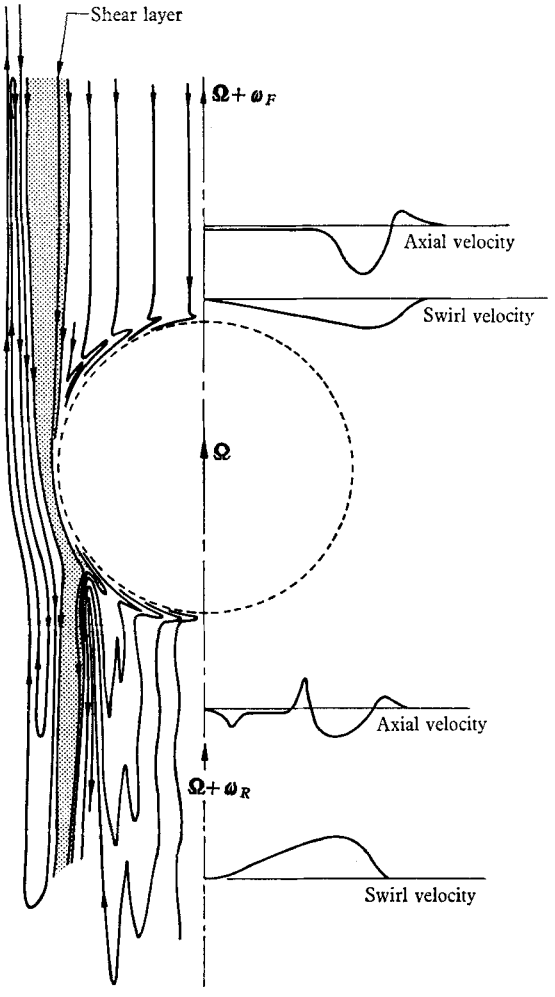

FIGURE 4. Meridional flow field around the sphere showing the acceleration within the shear layers and the anomalous boundary-layer behaviour behind the sphere.

To recapitulate, the forward 'Taylor' region loses fluid in *three* ways; through the Ekman layer on the sphere; through the Ekman layer on the upper plate, which in turn feeds an axial shear layer (an interaction described in more detail later); and through a small radial flow within the slug itself, an effect which is not a part of the M–S specification because of its inertial origin.

One of the most interesting features of the whole flow around the sphere is the appearance of the boundary-layer fluid as it is ejected from the rear of the sphere (figure 5, plate 1). This photograph, and many other like it taken under a wide

range of circumstances, is a little misleading and must be interpreted with some care. The boundary layer is very thin and the layer of dye is distributed through a finite portion of it from the sphere surface outwards. The dye particles furthest from the sphere are ejected into the outer flow first, as can be clearly seen in the photograph (figure 5, plate 1). In one revolution of the outer flow with respect to the sphere the particles travel an axial distance given by the pitch of the helix of dye.† Particles closer to the surface continue to move radially inwards until they too are ejected into the outer flow. The dye right at the sphere surface never reaches the pole of the sphere, as the corresponding Ekman layer solution requires, and the terminal flow out of the layer is characterized by a central region of stagnant fluid which is rotating slightly slower than the rest of the 'Taylor column'. Such behaviour is apparently typical of all layers of this convergent type‡ whether they are Ekman layers, as in the present case, or non-linear boundary layers, as reported in Bretherton, Carrier & Longuet-Higgins (1966, p. 395). Such layers present a variety of configurations depending on the nature of the outer flow (e.g. solid body-like rotation or vortex-like motion) and the fluid dynamic parameters (e.g. Taylor number, ratio of surface rotation speed to outer flow rotation speed), and will be reported on more fully in the future.

All of the cases suggest a situation for the present case like that shown diagrammatically in figure 9. Detailed features in other cases may be different, e.g. the vortex breakdown region may be many boundary-layer thicknesses in radius, or the stagnant region may in fact be strongly recirculating, etc.; but the general features and the qualitative description are essentially the same. Under the action of the external pressure gradient boundary-layer fluid moves inward continuously being vertically ejected into the outer region, as in the convergent Ekman layer solution. As it approaches the centre instead of terminating smoothly, as the theoretical solution shows, the fluid is forced into a high velocity, rapidly swirling axial jet which breaks down from an initially 'supercritical' state to a final slightly oscillatory 'subcritical' state. The increased axial velocity required to produce the initial supercritical flow is provided by the pressure field associated with the breakdown itself, which prevents the Ekman solution from occurring in its neighbourhood and diverts the fluid, that would have been expelled, into the central jet (cf. similar but more dramatic interaction between a tornado and the ground (Maxworthy 1967)). Why the flow prefers this condition to the smooth Ekman solution can only be answered from a solution of the unsteady problem since the steady Ekman solution allows no such breakdown. Work in related, unsteady boundary-layer flows shows that the initial solid body flow is changed by the inward motion of a vertical sheet of fluid across which the angular velocity changes rapidly and within which there is a large,

† The ratio of the pitch of the helix of dye to its circumference is a measure of the ratio of the axial velocity to the circumferential velocity in the Taylor column and can be used to find one of these velocities once the other is known.

‡ A convergent layer is here defined as one in which the boundary-layer fluid is moving inwards towards the centre of rotation and the outer flow has an axial velocity directed away from the layer.

vertical velocity (cf. Wedemeyer's (1964) solution for the related boundary-layer case). An annular vortex jump occurs where the large, vertical velocity leaves the boundary layer and as this converges onto the central axis it tends to the steady-state solution already described. In some boundary-layer flows it has been observed that this annular breakdown can remain stationary many boundary-layer thicknesses from the central axis, with the fluid outside rotating rapidly and the fluid inside not rotating at all!

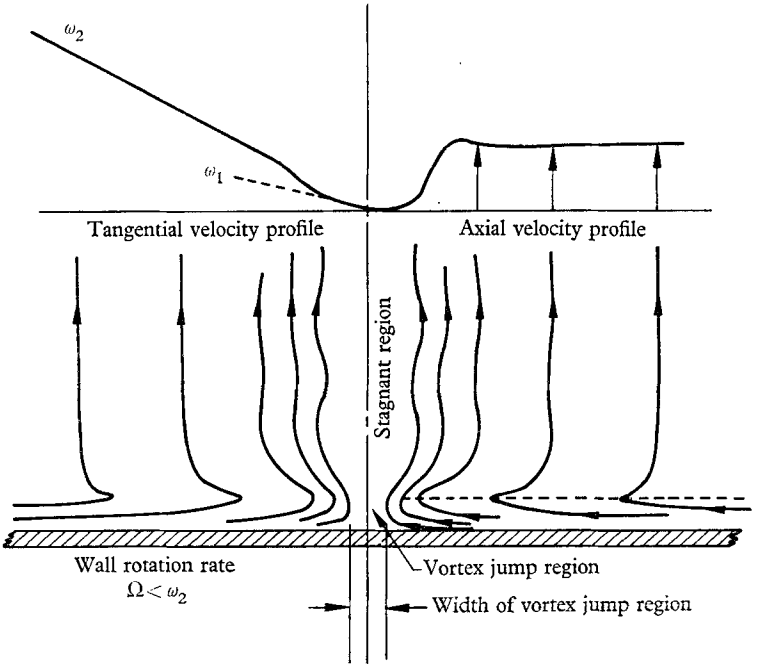

FIGURE 9. Diagrammatic view of the flow associated with a convergent Ekman layer.

In the present case, of course, this whole difficulty takes place over such a small central area that it has very little effect on such a gross parameter as the drag of the sphere, but it, nevertheless, points out an important deviation from the previously well thought of, but experimentally unverified, Ekman solution. Once this fluid has left the rear of the sphere, its travels are not yet complete because it also helps to feed the vertical shear layers, as shown in figure 4.

The interactions occurring in the end wall layers must also be discussed separately because one, the upper, is absorbing fluid while the other is ejecting fluid and displays all of the difficulties described previously for the layer behind the sphere. Thus fluid comes from above through the surrounding shear layer, converges towards the centre and goes through the same breakdown as the rear sphere layer. The interaction at the upper end plate is apparently well behaved with fluid being absorbed uniformly into the Ekman layer and then re-emitted into the surrounding shear layers. There is a vague but virtually unprovable indication that the fluid being ejected into this shear layer also goes through an annular vortex jump, but the motions are so slow and difficult to observe that this must

remain a subject for further study (figure 6*a*, plate 2). Also in the category of future observations is the whole problem of instability of the vertical shear layers and eventually of the interior of the Taylor column itself. A few observations suggest that the condition to the right of the break in the curve of figure 3 occurs when the whole interior of the Taylor column becomes unstable (figure 8*a*, plate 4). To the left only the outermost region of the vertical shear layers is unstable, but insufficient evidence is available to make a more satisfactory statement. The instability is undoubtedly of the same type as that observed by Hide & Titman (1967) in the related problems of differential rotation of concentric spheres and coaxial disks.

When the upper surface is free, the previous discussion concerning the Ekman layers around the sphere and at the lower, solid wall are qualitatively unchanged. However, for the range of these experiments the region between the sphere and the free surface contains a feature which was only slightly in evidence in the previous case. A column of dye injected along the axis instead of being absorbed entirely by the Ekman layer now becomes shortened and fattened by the flow until it fills the Taylor column (figures 7*a*, *b*, plate 3). There is a large radial flow within the whole column which is only explainable by allowing the existence of considerable inertial effects to replace the missing Ekman layer, and the radial flow short circuits much of the flow past the Ekman layer on the sphere (figures 7*a*, *b*, plate 3). This partially explains why this case has only a slightly increased drag over the previous case and is far from the theoretical asymptote, especially at large Reynolds numbers. As already noted, a similar effect occurs when the sphere rises towards a solid wall and accounts for part of the difference between the measured drag and the results of the simplified theory with negligible inertial effects.

Quantitative velocity measurements

Using the 'indicator' technique described by Baker (1966) and the apparatus shown in figure 1*b*, it was possible to measure the azimuthal velocity profiles in the two wakes. All axial velocities are so much smaller, that it is impossible to measure their magnitude and we use the technique only to determine their direction at various radial locations. Figure 8*b*, plate 4, shows such a profile for the forward slug with parameter values, $R = 14$, $T = 4200$, one revolution of the tank after the dye was initially created. Solid body rotation with angular velocity ω exists at the centre; this was measured and used in the construction of figure 10. Theoretically this central rotation rate is proportional to $RT^{-\frac{1}{2}}\Omega$, and the theoretical asymptote on the ordinate of figure 10 is $\frac{1}{2}$. Results are plotted only versus R, because the scatter is too great to try to make a further reduction as we could with the drag results. The fore-and-aft asymmetry of the flow is marked and is only reduced as inertia effects become small. This asymmetry also shows up in measurements of the wake width, the forward wake being slightly wider than the rearward one, in confirmation of the dye studies and the reconstruction of figure 4. Observations of the shape of the velocity profiles in the shear layers themselves are obscured by sphere curvature effects as discussed

in M–S, so that the inner transition from slug solid body rotation is very slow. The outer transition from shear layer to the solid body rotation rate of the tank is very rapid and is probably more typical of the changes that take place in such layers. Experiments using a moving disk, with no body curvature effects, should be more enlightening than the present results on this point.

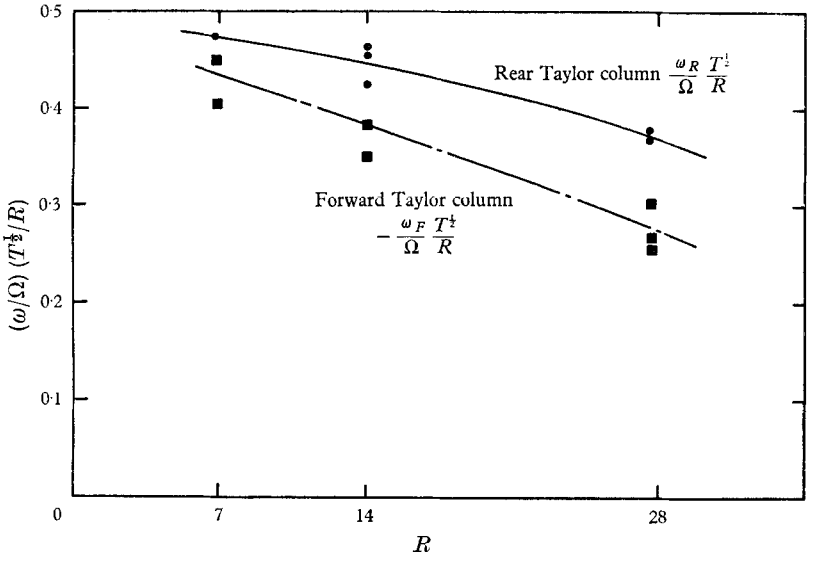

FIGURE 10. $(\omega/\Omega)(T^{\frac{1}{2}}/R)$ versus R for $4000 < T < 16{,}000$. The rotation rate of both fore $(-w_f)$ and aft (w_R) slugs compared to the theoretically predicted value. Ω is direction of positive rotation.

Conclusions

Can be summarized as follows.

(i) We have determined the motion of a sphere as it rises through a rotating tank of water of finite length; by measuring its velocity of rise for various diameters, buoyancy forces and rotation rates and calculating the drag coefficient; by observing the motion of dye introduced into various locations; and by measuring the azimuthal velocity profiles in the fore and aft slugs.

(ii) The drag coefficient measurements show that the results of Moore & Saffman (1968) are approached when inertia forces everywhere in the flow are very much smaller than both viscous and Coriolis forces.

(iii) Dye motion studies have indicated several locations where inertia effects are important: in the shear layers as they thin and support an annular vortex breakdown in the neighbourhood of the sphere equator; in the forward slug within which there is a radial flow of inertial origin; in the boundary-layer flow being ejected into the rearward slug at both the sphere and the lower solid boundary.

(iv) Both dye studies and azimuthal velocity measurements show a marked fore and aft asymmetry in the flow which is a further manifestation of these finite inertial effects in the range of parameters studied.

(v) Tests with an upper free surface indicate a drag coefficient which is larger than that found with a solid upper surface at the same values of all the parameters.

Many rewarding discussions with Drs D. W. Moore and P. G. Saffman are gratefully acknowledged. D. E. Griffith constructed the apparatus and suggested many subtle improvements; without his aid the results would have been infinitely harder to obtain.

This paper presents the results of one phase of research carried out at the Jet Propulsion Laboratory, California Institute of Technology, under Contract no. NAS7-100, sponsored by the National Aeronautics and Space Administration.

REFERENCES

BAKER, J. 1966 A technique for the precise measurement of fluid flow in the range 0–5 cm/sec. *J. Fluid Mech.* **26**, 3.

BENJAMIN, T. B. 1962 Theory of the vortex breakdown phenomenon. *J. Fluid Mech.* **14**, 4, 593.

BRETHERTON, F. P., CARRIER, G. F. & LONGUET-HIGGINS, M. S. 1966. Report on the I.U.T.A.M. symposium on rotating fluid systems, *J. Fluid Mech.* **26**, 2, 393.

HIDE, R. & TITMAN, C. W. 1967 Detached shear layers in a rotating fluid. *J. Fluid Mech.* **29**, 1.

MAXWORTHY, T. 1967 The flow creating a concentration of vorticity over a stationary plate. *JPL Space Programs Summary*, no. 37–44, vol. IV.

MOORE, D. W. & SAFFMAN, P. G. 1968 The rise of a body through a rotating fluid in a container of finite length. *J. Fluid Mech.* **31**, 635.

TAYLOR, G. I. 1923 The motion of a sphere in a rotating fluid. *Proc. Roy. Soc.* A **102**, 180.

WEDEMEYER, E. H. 1964 The unsteady flow within a spinning cylinder. *J. Fluid Mech.* **20**, 3, 383.

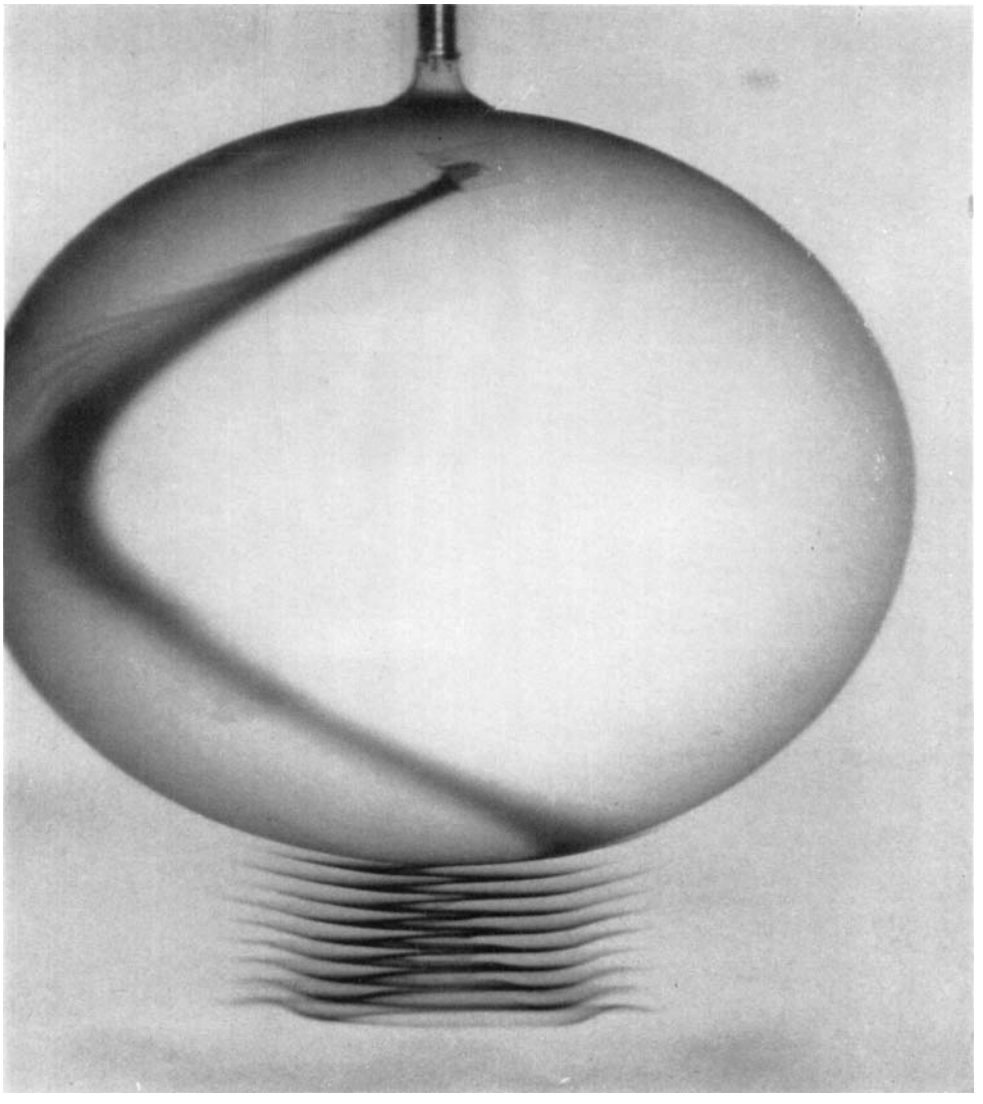

FIGURE 5. Flow in the Ekman layers around the sphere. $T = 15{,}900$; $R = 28$. Dye introduced into a finite portion of the Ekman layer on the upper hemisphere travels around to the rear hemisphere where it is ejected in the form of a helix. Note that dye particles never reach the pole of the sphere as required by the corresponding Ekman boundary-layer solution.

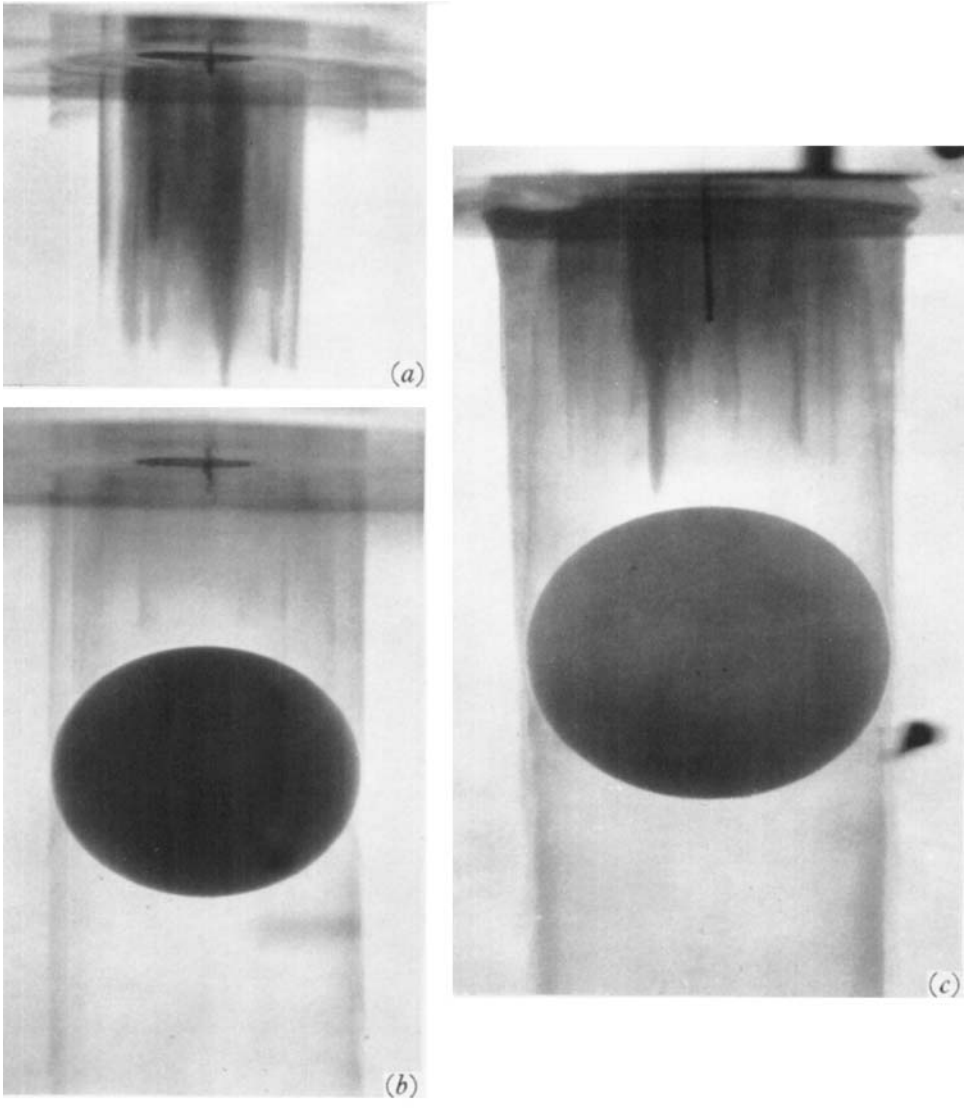

FIGURE 6 (*a*) and (*b*). The change in the shape of a dye column introduced ahead of a rising sphere. Note the dye flow away from the upper wall in (*a*), and the change in diameter of the column of dye. $T = 12{,}000$; $R = 9{\cdot}5$. (*c*). Showing a thinning of the shear layer and the clear division between fluid in this layer and that within the central region. $T = 8400$; $R = 15{\cdot}5$.

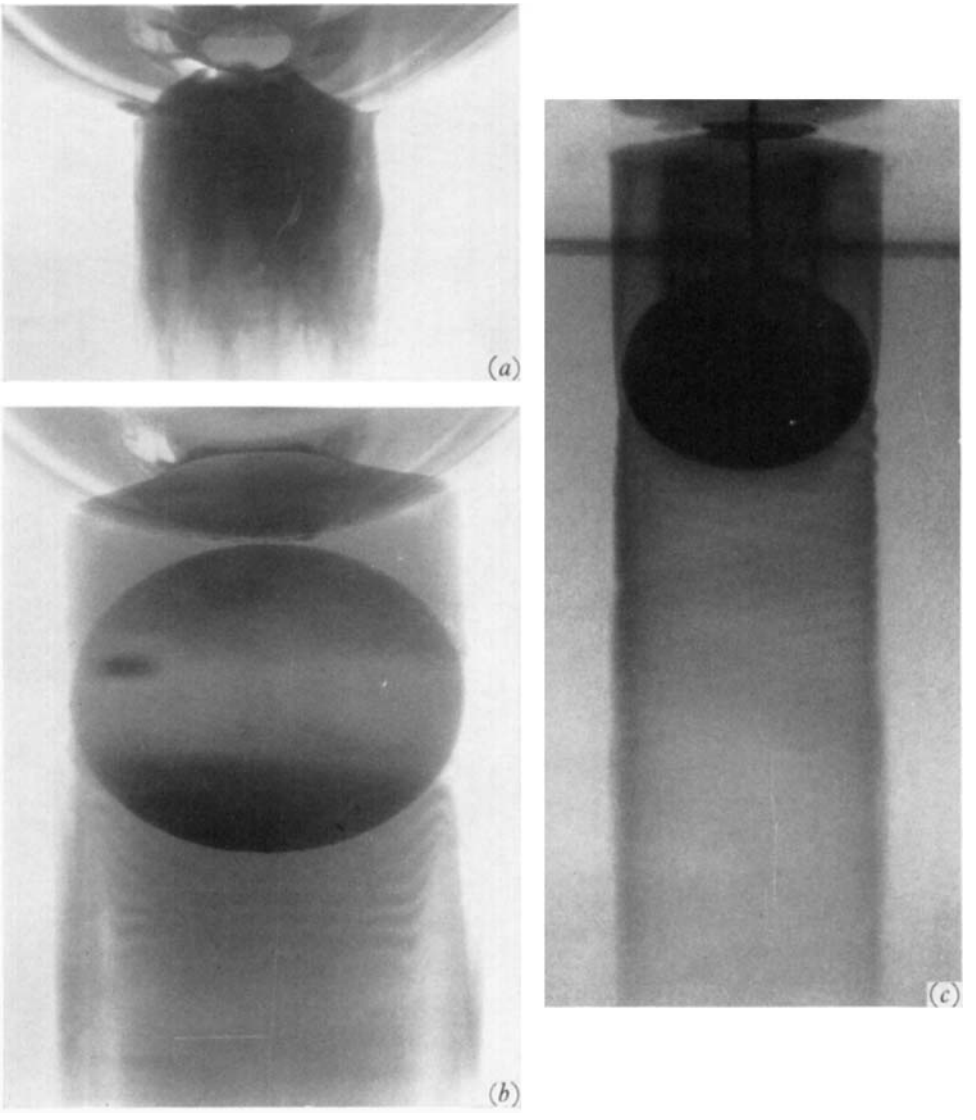

FIGURE 7 (*a*) and (*b*). Showing radial flow and absence of shear layers in forward slug with an upper free surface. Note evidence of reversed flow in the rear slug. $T = 17{,}900$; $R = 4{\cdot}4$. (*c*). Undular vortex breakdown in the annular shear layer as it accelerates past the sphere equator. Note wavelike motions in the shear layers. $T = 5900$; $R = 33{\cdot}2$. Topmost image is a reflexion from the upper wall, dark line is the dye injection tube.

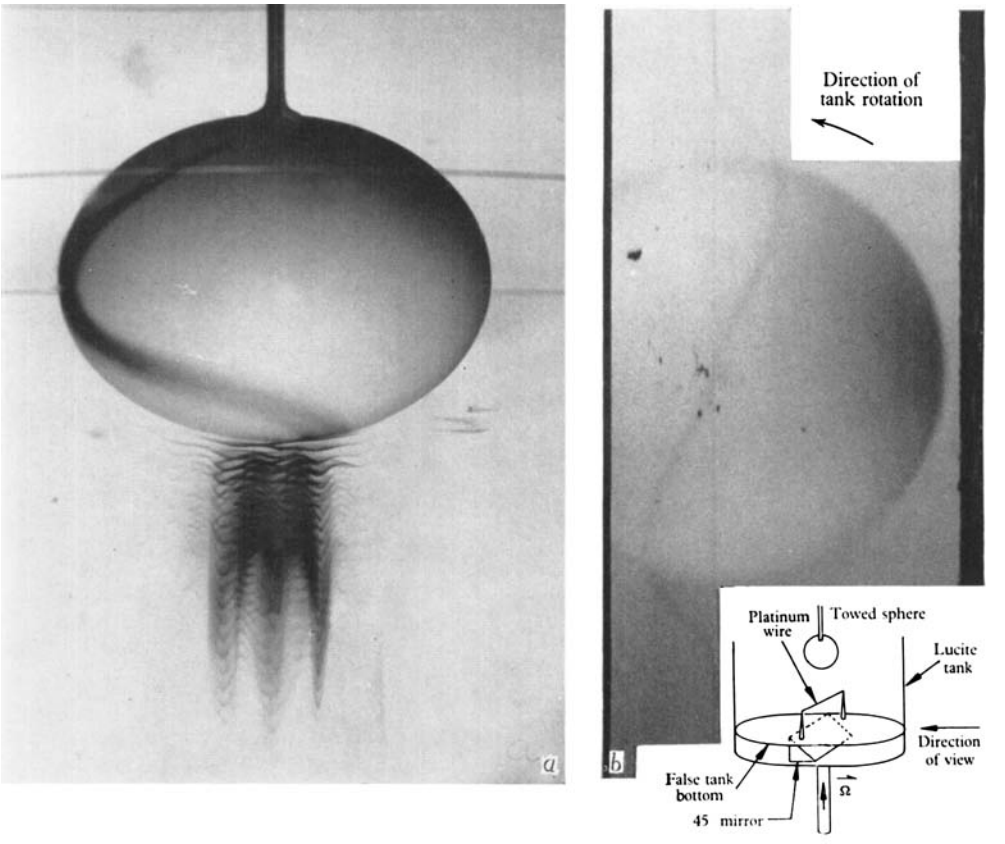

FIGURE 8 (*a*). Azimuthal instability of the rear slug when $R/T^{\frac{1}{3}}$ exceeds unity, actually 1·3. (*b*). Swirl velocity profile in forward slug, one diameter ahead of the sphere, one revolution of the tank after the dye line was formed. $T = 4200$; $R = 14$. Inset shows geometric configuration for this photograph.